


ORIGINAL ARTICLE

Electric-field penetration depth and dielectric spectroscopy observations of human skin

Yuko Maruyama¹  | Hayato Kamata² | Seiei Watanabe² | Rio Kita³ | Naoki Shinyashiki³ | Shin Yagihara³

¹Graduate School of Science and Technology, Tokai University, Hiratsuka, Kanagawa, Japan

²Graduate School of Science, Tokai University, Hiratsuka, Kanagawa, Japan

³Department of Physics, School of Science, Tokai University, Hiratsuka, Kanagawa, Japan

Correspondence

Shin Yagihara, Department of Physics, School of Science, Tokai University, 4-1-1 Kitakaname, Hiratsuka, Kanagawa 259-1292, Japan.
Email: yagihara@keyaki.cc.u-tokai.ac.jp

Abstract

Background: The dynamic behavior of water molecules remains an important subject for understanding human skin. The change in the dynamics of water molecules from those in bulk water can be effectively observed by dielectric spectroscopy. To study water in the human skin in vivo, non-invasive and non-destructive measurements are essential. Since many unknowns remain from previous research, in this report we employ a two-layer dielectric model to evaluate the penetration depth of the electric field and use the results in measurements on human skin.

Materials and Methods: We used open-ended coaxial probes with different diameters to perform time-domain reflectometry (TDR) measurements for an acetone-Teflon double-layer model and for human skin from various parts of the body.

Results: The electric-field penetration depth obtained from model measurements increases with the increasing outer diameter of open-ended coaxial electrodes. For skin measurements, the relaxation strength corresponding to the water content shows a clear dependence on the epidermal thickness of the measured body parts.

Conclusion: We determined the depth distribution of the water content of skin from results of dielectric measurements obtained using electrodes with various electric-field penetration depths. We found exponential decays with the thickness of the epidermis of each body part for several examinees. This study suggests an effective method for detailed evaluations of human skin.

KEYWORDS

dielectric measurement, epidermis, human skin, water content

1 | INTRODUCTION

The characteristics of biological materials are closely related to their water content. Consequently, measurements of the dynamics of water molecules are important in order to understand the structures of hydrous materials and their biological functions. Human skin is composed of three layers termed, sequentially inward from the surface, the epidermis, dermis, and subcutaneous tissue. The water

content of the epidermis is lower than that of the dermis,^{1,2} and it behaves as a protective barrier against drying and external irritation. The existence of bound water³⁻⁸ is often suggested, even for human skin.⁹ It is not easy to determine the variation of the water content with depth, and measurements are difficult, since water molecules exhibit complex variations on different temporal and spatial scales.

Dielectric measurements using time-domain reflectometry (TDR) make it possible to observe relaxation processes that reflect

This is an open access article under the terms of the Creative Commons Attribution-NonCommercial-NoDerivs License, which permits use and distribution in any medium, provided the original work is properly cited, the use is non-commercial and no modifications or adaptations are made.

© 2019 The Authors. *Skin Research and Technology* Published by John Wiley & Sons Ltd

the molecular motions of water. The relaxation process is caused by the formation and disappearance of dynamic clusters of water molecules. For free water molecules, the relaxation time is $\tau = 8.27$ ps at 25°C.¹⁰⁻¹³ This relaxation time is generally smaller than that of biological macromolecules.

The water content of human skin has been studied extensively by various methods.¹⁴⁻¹⁶ Pratchyapruit et al¹⁷ suggest that the skin of the eyelid remains soft by maintaining sufficient hydration on the skin surface. This example demonstrates that water in the skin is related to biological function.

In our previous studies, we obtained information about the dielectric properties in the stratum corneum of human skin.^{18,19} We also have reported that the healing of human skin after a burn is correlated with the time dependence of its free water content.²⁰ Applying dielectric measurements of skin to the area of sports medical science, we were able to observe the large-scale traversal of water molecules into the body during exercise.²¹ Dielectric spectroscopy can be employed for non-invasive and non-destructive measurements, including in vivo measurements of human skin. These reports clearly indicate that skin measurements using dielectric spectroscopy can provide an important method for characterizing the state of the skin through observations of the molecular behavior of water.

Recently, measurements of the moisture content of skin have been performed using confocal Raman spectroscopy.²² This experimental technique makes it possible to observe the moisture content at a shallow depth in areas of the skin such as the stratum corneum and epidermis. On the other hand, dielectric spectroscopy yields a value averaged over the penetration depth of the electric field up to the skin surface contacted by the electrode. Furthermore, by

increasing the electrode diameter it is possible to obtain information in deeper areas than can be studied with confocal Raman spectroscopy. We have previously reported a comparison of results obtained from these two measuring techniques.²³ Observations of the dynamics of water molecules using dielectric spectroscopy are relevant not only to the water content but also to phenomena such as biological functions and characteristics in vivo. Therefore, dielectric spectroscopy is appropriate for in vivo measurements.

In dielectric spectroscopy of the skin, it is important to know which and how dielectric information in depth is obtained for substances with different water contents. Accordingly, we have examined the characteristic electric-field penetration depths of a two-layer dielectric model using water and a Teflon block.^{18,24,25} The penetration depth obtained from such measurements depends on the outer diameter of the coaxial electrode. However, the electrode diameter was only one of the unknowns in previous research. In this study, we have used TDR with open-ended coaxial electrodes having different electric-field penetration depths to perform dielectric measurements of an acetone-Teflon double layer and of human skin from various parts of the body, in order to study the distribution of water content in the human skin.

2 | MATERIALS AND METHODS

2.1 | Acetone-Teflon double-layer system for the characterization of coaxial electrodes

A block diagram of the apparatus employed for the characterization of coaxial electrodes is shown in Figure 1. We purchased a flat, 10-mm-thick Teflon sheet with static permittivity $\epsilon_t = 2.1$ from FLON INDUSTRY. We placed a glass bottle on a jack and filled the bottle with acetone (with static permittivity $\epsilon_a = 21$ at 20°C²⁶). We then placed a Teflon sample in the bottom of the bottle to form an acetone-Teflon double-layer system. We first placed the end of the electrode into contact with the surface of the Teflon, and we then changed the vertical distance between the Teflon surface and the end of the electrode gradually using the jack while we performed the dielectric measurements. We determined the distance using a digital indicator. We used 50 Ω , semi-rigid coaxial cables (SUHNER) with outer diameters of 0.86, 1.19, 2.20, 3.56, and 6.35 mm as the electrodes for the TDR measurements at room temperature (20.0 \pm 0.5°C).

2.2 | Human skin measurements on various parts of a body

We measured various parts of the bodies of two examinees (A: male, age 24; B: female, age 26) using TDR, with the same electrodes as we used for the acetone-Teflon double-layer measurements at room temperature, 20.0 \pm 0.5°C, with humidity 50 \pm 1%. The body parts we measured were the cheek, the palm side of the forearm, the palm, and the sole of the foot. We also used TDR to measure the same body parts of two other examinees (C: male, age 24; D: female, age 22) with an electrode having an outer diameter of 2.2 mm. We

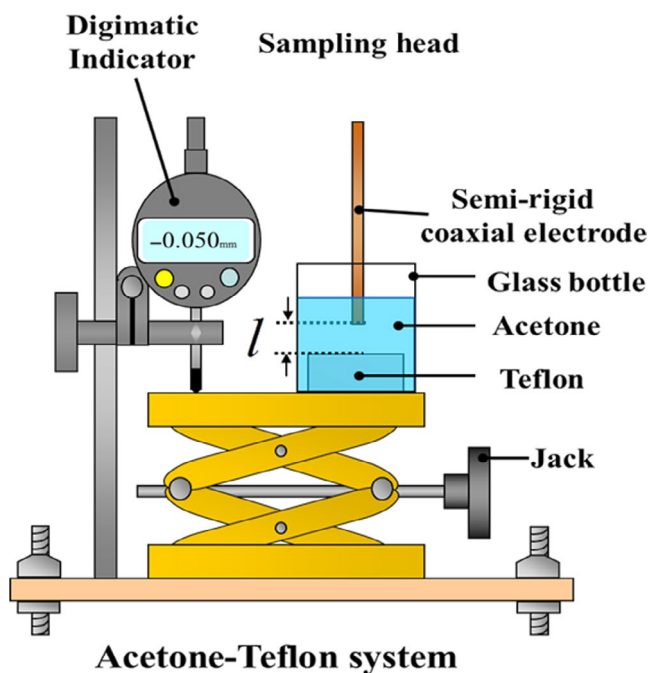


FIGURE 1 Block diagram used for the acetone-Teflon double-layer measurements [Colour figure can be viewed at wileyonlinelibrary.com]

TABLE 1 Values of correction coefficients

ϕ [mm]	0.86	1.19	2.20	3.56	6.35
γd [mm]	0.059	0.082	0.15	0.29	0.46

washed the measured body parts with soap and wiped them with Kimwipe before the measurements. In order to restore the state of the skin prior to the measurements, we asked each examinee to remain still in the examining room for 30 minutes so as not to sweat.

2.3 | Time-domain reflectometry measurements

We employed a digitizing oscilloscope mainframe (HP 54120B) with a four-channel test set (HP 54124A) as the TDR system.²⁷⁻³¹ This enabled us to make dielectric measurements—especially for the relaxation process due to the molecular dynamics of free water—over the frequency range from 100 MHz to 30 GHz. We observed the reflected microwave signals, which include information about the dielectric properties of the sample in response to the incident step pulse.

The complex permittivity of the sample can be expressed by the basic equation of the TDR method:²⁷⁻²⁹

$$\epsilon^* = \frac{c'}{j\omega\gamma d} \frac{v_0 - r}{v_0 + r} X \cot X \quad (1)$$

where c' is the speed of propagation in the coaxial line, v_0 and r are the Laplace transforms of the incident and reflected pulse waveforms, $X \cot X$ takes into account propagation and multiple reflections in the sample and the coaxial line geometry, and γd is a correction coefficient. There is reference method²⁷⁻²⁹ using the difference between the reflected wave of a standard sample having a known complex dielectric constant and the reflected wave of an unknown sample, which was used because it is more accurate.²⁷⁻²⁹ The values of the correction coefficients γd are listed for each electrode in Table 1. We also calibrated the open-ended probes using standard samples (air, acetone, and water) with known dielectric properties.

We performed the TDR measurements using a contact-type coaxial electrode with an open-ended tip in direct contact with the object to be measured. The TDR measurement requires an electric field generated around the tip of the electrode. The electric lines of force reach from the central to the outer conductors through the interior of

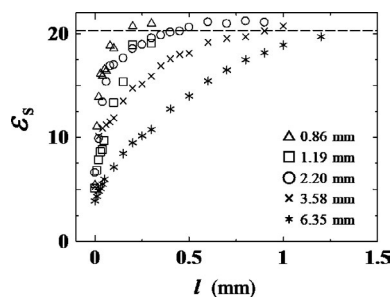


FIGURE 2 Relationship of the measured dielectric constant to the distance between the Teflon surface and the electrode, for outer electrode diameters of 0.86, 1.19, 2.20, 3.58, and 6.35 mm

TABLE 2 Parameters for an electrode with an outer diameter of 0.86 mm

l [mm]	ϵ_s	$\ln(\epsilon_a - \epsilon_s)$
0.00	5.43	2.75
0.01	11.04	2.30
0.02	13.91	1.96
0.03	16.13	1.58
0.04	15.91	1.63
0.05	16.53	1.50
0.06	16.40	1.53
0.08	18.83	0.78
0.10	18.56	0.89
0.20	20.70	-1.21
0.30	20.97	-3.44

the object. The dielectric information is obtained in the region where a relatively large electric field is applied around the electrode tip. Therefore, the electric lines of force necessarily depend on the diameter of the electrode. In this report, we use measurements of the dielectric information averaged over the penetration depth of the electric field as the basis for discussing the layered structure of the human skin.

3 | RESULTS

3.1 | Acetone-Teflon double-layer system

Figure 2 shows the relationship between the static dielectric constant ϵ_s and the distance l between the electrode and the Teflon surface for electrodes with outer diameters of 0.86, 1.19, 2.20, 3.56, and 6.35 mm. The ϵ_s values increase with increasing l , and they asymptotically approach the value for acetone. The dielectric constant thus obtained is larger than $\epsilon_t = 2.1$, even when the end of electrode just touches the Teflon surface ($l = 0$), because there remains a small gap filled with acetone. The variation of the dielectric constant with position thus obtained shows exponential-like decays.

TABLE 3 Parameters for an electrode with an outer diameter of 1.19 mm

l [mm]	ϵ_s	$\ln(\epsilon_a - \epsilon_s)$
0.00	5.11	2.77
0.01	6.82	2.65
0.02	7.81	2.58
0.03	8.58	2.52
0.04	8.81	2.50
0.05	9.66	2.43
0.10	13.34	2.04
0.15	15.33	1.74
0.20	18.91	0.74
0.25	19.07	0.66

3.2 | Human skin measurements

We used electrodes with various outer diameters to measure various parts of the body, and we observed the respective dielectric relaxation curves. We found the dielectric constant to be small when the electrode diameter was small. In addition, we obtained smaller values of the dielectric constant for body parts with larger skin thicknesses.

4 | DISCUSSION

4.1 | Characterization of the penetration depth of the electric field

The distance dependence shown in Figure 2 can be expressed approximately by the following equation:^{24,25}

$$\varepsilon_s = \varepsilon_t - \left\{ \varepsilon_a - \varepsilon_t \left[1 - \exp\left(-\frac{l}{l_0}\right) \right] \right\}, \quad (2)$$

where ε_a is the dielectric constant of acetone, and l_0 is defined as the penetration depth of the electric field. The penetration depth has a characteristic value for each electrode, which is determined from Equation 2. The penetration depth is an average value, and some parts of the electric field lines reach deeper regions.

The dielectric constant ε_s and the distance l thus obtained are listed in Tables 2-6. As noted in Section 3.1 above, when the end of the electrode just touches the Teflon surface ($l = 0$), the dielectric

TABLE 4 Parameters for an electrode with an outer diameter of 2.20 mm

l [mm]	ε_s	$\ln(\varepsilon_a - \varepsilon_s)$
0.00	6.62	2.67
0.02	9.89	2.41
0.04	13.41	2.03
0.06	15.36	1.73
0.08	16.88	1.42
0.10	17.00	1.39
0.15	17.63	1.21
0.20	18.53	0.90
0.25	18.93	0.73
0.30	19.57	0.36
0.35	19.83	0.16
0.40	20.12	-0.13
0.45	20.22	-0.25
0.50	20.60	-0.92
0.60	21.10	-
0.70	20.95	-3.00
0.80	21.19	-
0.90	21.07	-

TABLE 5 Parameters for an electrode with an outer diameter of 3.58 mm

l [mm]	ε_s	$\ln(\varepsilon_a - \varepsilon_s)$
0.00	5.27	2.76
0.02	10.11	2.39
0.04	10.89	2.31
0.06	11.22	2.28
0.08	11.49	2.25
0.10	11.88	2.21
0.15	13.50	2.01
0.20	14.74	1.83
0.25	15.12	1.77
0.30	15.90	1.63
0.35	16.89	1.41
0.40	17.55	1.24
0.45	17.98	1.11
0.50	18.1	1.06
0.60	19.15	0.62
0.70	19.51	0.40
0.80	19.7	0.26
0.90	20.24	-0.27
1.00	20.74	-1.35

constant obtained from the measurements is larger than $\varepsilon_t = 2.1$ because of acetone in the gap between the end of the electrode and the Teflon surface. In our previous research, we pointed out that

TABLE 6 Parameters for an electrode with an outer diameter of 6.35 mm

l [mm]	ε_s	$\ln(\varepsilon_a - \varepsilon_s)$
0.00	3.90	2.84
0.01	4.35	2.81
0.02	4.85	2.78
0.03	5.08	2.77
0.04	5.51	2.74
0.05	5.97	2.71
0.10	7.15	2.63
0.15	8.45	2.53
0.20	9.48	2.44
0.25	10.16	2.38
0.30	10.76	2.33
0.40	12.74	2.11
0.50	13.98	1.95
0.60	15.43	1.72
0.70	16.49	1.51
0.80	17.47	1.26
0.90	18.14	1.05
1.00	18.90	0.74
1.20	19.69	0.27

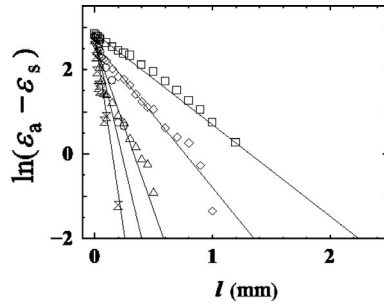


FIGURE 3 Approximation lines in semi-logarithmic plots for various electrodes. The symbols are the same as in Figure 2

this does not affect our determination of the penetration depth, as explained below.^{24,25} Equation 2 can be rewritten as

$$\varepsilon_a - \varepsilon_s = (\varepsilon_a - \varepsilon_t) \exp\left(-\frac{l}{l_0}\right), \quad (3)$$

which corresponds to a straight line in the semi-logarithmic plot shown in Figure 3. We obtained these straight lines from least-squares fits to the exponential function given by Equation 3 for each electrode diameter. The slope of this straight line gives the electric-field penetration depth l_0 . The penetration depth so obtained for each electrode diameter is listed in Table 7. The penetration depth clearly increases with increasing electrode diameter. This diameter dependence is reasonable, because the electric field lines from the central to the outer conductors are longer for electrodes with larger outer diameters.

4.2 | Human skin observed using dielectric spectroscopy

Dielectric relaxation spectra obtained from TDR measurements of the palm side of the forearm using electrodes of various diameters are shown in Figure 4. The curves show at least two relaxation processes, one in the frequency region above 10 GHz and the other below 1 GHz. Figure 4 also shows that larger dielectric constants and losses are obtained for electrodes with larger diameters.

The dielectric relaxation curves thus obtained can be described by the sum of two Cole-Cole equations:

$$\varepsilon^* = \varepsilon_\infty + \frac{\Delta\varepsilon_h}{1 + (j\omega\tau_h)^\beta} + \frac{\Delta\varepsilon_l}{1 + (j\omega\tau_l)^\beta}, \quad (4)$$

where ε^* is the complex dielectric permittivity, ε_∞ is the high-frequency limit of the dielectric constant, $\Delta\varepsilon$ is the relaxation strength, τ is the relaxation time, β is the relaxation time distribution parameter, and h and l indicate the higher and lower relaxation processes,

TABLE 7 Penetration depth of the electric field

ϕ [mm]	0.86	1.19	2.20	3.56	6.35
l_0 [mm]	0.052	0.11	0.15	0.30	0.49

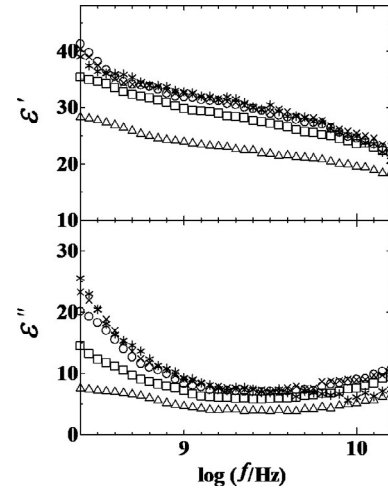


FIGURE 4 Frequency dependence of the complex dielectric constant of human skin obtained using various probe diameters. The symbols are the same as in Figure 2

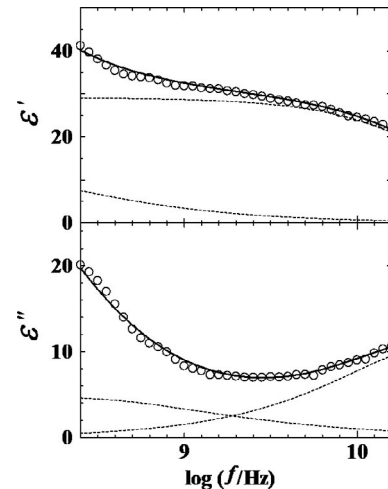


FIGURE 5 Frequency dependence of the complex dielectric constant obtained with an electrode having an outer diameter of 2.20 mm. The solid lines correspond to the two relaxation processes obtained from the fitting procedure

respectively. A typical result of a fit of Equation 4 to the relaxation processes obtained for the palm side of the forearm using the 2.20 mm-diameter electrode is shown in Figure 5. It is reasonable to assume that the h process results from the reorientation of free water molecules and that the l process results from a superposition of multiple factors, such as interfacial polarization, bound water, and local chain motions of macromolecules, as indicated in our previous work.²⁰

Figures 6 and 7 show the relationship between the relaxation strength of the h process and the thickness d of the epidermis for two examinees. We obtained the thickness of the epidermis at the various measurement sites from the literature on anatomically based thicknesses,³² as listed in Table 8. The actual thickness of the epidermis for each examinee will in fact be different. Plots of the logarithm of $\Delta\varepsilon$ obtained for each electrode, however, showed straight

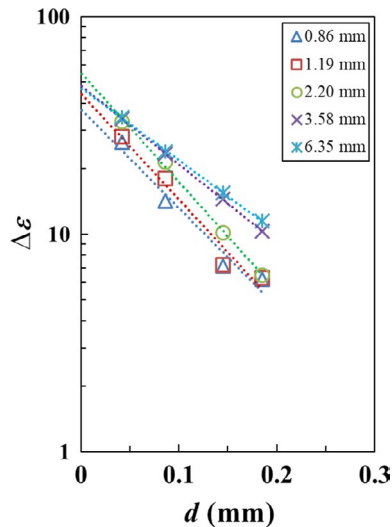


FIGURE 6 Relationship of the relaxation strength and the thickness of the epidermis for probes with outer diameters of 0.86, 1.19, 2.20, 3.58, and 6.35 mm [examinee A: male] [Colour figure can be viewed at wileyonlinelibrary.com]

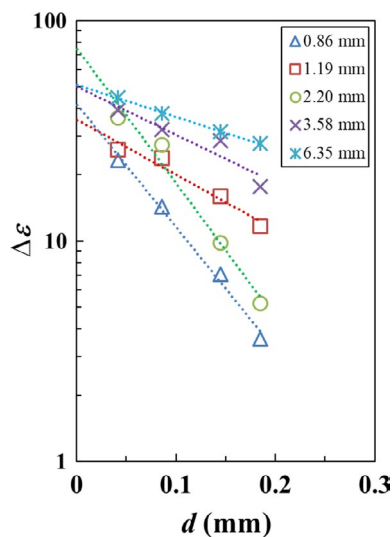


FIGURE 7 Relationship of the relaxation strength and the thickness of the epidermis for probes with outer diameters of 0.86, 1.19, 2.20, 3.58, and 6.35 mm [examinee B: female] [Colour figure can be viewed at wileyonlinelibrary.com]

lines against d , as shown in Figures 6 and 7. Though the relaxation strength depends on both the examinee and the physical conditions, Figures 6 and 7 indicate that this linear dependence is common and suggest that any such influence is small compared with the difference among the measured body parts.

In addition, we found that the thickness of the epidermis was neither extremely thin nor extremely thick compared to the average value for each measured body part, even for examinees. The straight lines show the dependence on the thickness of the body part of each examinee. Figure 7 shows that the straight lines for electrodes with larger penetration depths generally have

TABLE 8 Thickness of the epidermis of different body parts, from Ref. ³²

Body parts	Thickness of epidermis [mm]
Cheek	0.042
Palm side of the forearm	0.086
Palm	0.145
Sole of the foot	0.185

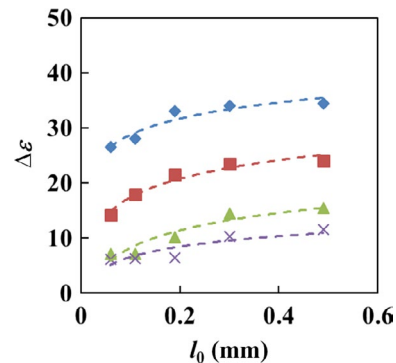


FIGURE 8 The moisture content of the skin of the cheek (\diamond), palm side of the forearm (\square), palm (\triangle), and the sole of the foot (\times) obtained from electrodes with different values of I_0 [examinee A: male] [Colour figure can be viewed at wileyonlinelibrary.com]

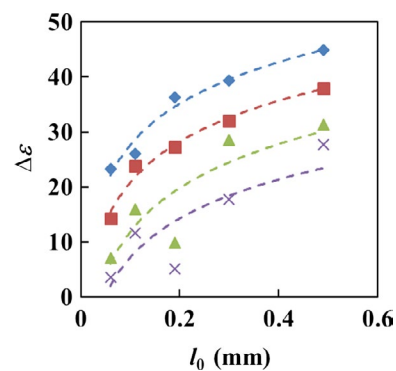


FIGURE 9 The moisture content of the skin of the cheek (\diamond), palm side of the forearm (\square), palm (\triangle), and the sole of the foot (\times) obtained from electrodes with different values of I_0 [examinee B: female] [Colour figure can be viewed at wileyonlinelibrary.com]

shallower slopes and larger values of the relaxation strength $\Delta\epsilon$ than those shown in Figure 6. This means that the contribution of dermis with high water content is smaller in Figure 6. Therefore, it is conceivable that examinee A (Figure 6) has a thicker epidermis than examinee B (Figure 7).

The vertical axes of Figures 8 and 9 represent the moisture content of the skin for each body part obtained by all electrodes, with different electric-field penetration depths I_0 . Electrodes with larger I_0 values apparently probe regions with larger moisture content, since the ratio of water-rich dermis to water-poor epidermis increases with I_0 . These curves show that examinee A exhibited

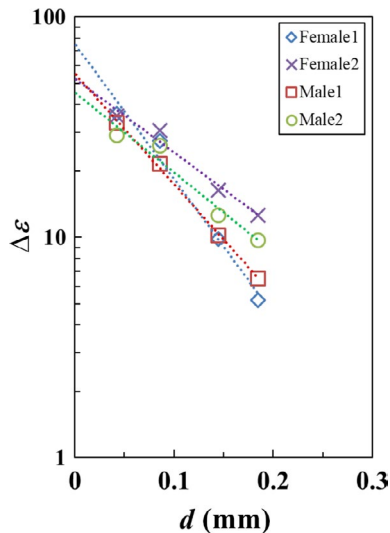


FIGURE 10 Relationship of the relaxation strength to the thickness of the epidermis for the probe with 2.2 mm outer diameter for four examinees, two males and two females [Colour figure can be viewed at wileyonlinelibrary.com]

less change in water content, compared with examinee B, because of the former's thicker epidermis. For examinee A, with a thicker epidermis, even if the penetration depth of the electrode increases, the apparent moisture content does not increase much. In other words, the present technique of dielectric spectroscopy can determine the unknown thickness of the epidermis of any body part.

Figure 10 shows the relationship between the relaxation strength of the h process and the thickness of the epidermis for the 2.20 mm-diameter electrode for four examinees. We found that for a given electrode diameter the difference in the slope depends on the examinee. This difference in the slope of the straight line expresses the difference in the thickness of the epidermis for each examinee. These results also depend on the physical condition of the day, however, although the effect is small compared to the difference between different body parts. Even if the thickness of the epidermis depends on the examinee, it is neither extremely thin nor extremely thick compared to the average value for each body part, as in Figures 6 and 7. Thus, the relative thickness of each body part exhibits a linear dependency for each examinee. The thickness of human skin thus does not change drastically between different parts of the body. These results demonstrate that our present approach can be an effective tool for a detailed assessment of human skin.

5 | CONCLUSION

We determined the penetration depths of the electric fields of open-ended coaxial electrodes of various diameters that we used for dielectric measurements. The penetration depth increases with increasing electrode diameter. We found from systematic measurements with various electrodes that the epidermis has a

more limited water content than the dermis. The logarithm of the relaxation strength obtained for each electrode follows a linear relationship with the thickness of the epidermis in the different examinees. The differences in slope of the straight lines correspond to differences in the thickness of the epidermis of the examinees. Even if the thickness of the epidermis depends on the examinee, the relative thickness of each part generally offers the linear dependency, as it is neither extremely thin nor extremely thick compared to the average value of each part. These characteristic behaviors suggest a methodology for a detailed assessment of the skin using the present analysis of systematic dielectric measurements with coaxial electrodes having different penetration depths.

ACKNOWLEDGMENTS

We are grateful to Hayaka Torada for generously providing us with part of experimental data and Figure 1 drawing. We also appreciate Tatsuya Goto for providing Figure 1 setup and drawing.

ORCID

Yuko Maruyama  <https://orcid.org/0000-0001-8341-1566>

REFERENCES

1. Abe T. Water and the skin. *J Jpn Oil Chem Soc.* 1985;34:413-419.
2. Tagami H. Electrical measurement of the hydration state of the skin surface in vivo. *Br J Dermatol.* 2014;171:29-33.
3. Umehara T, Kuwabara S, Mashimo S, et al. Dielectric study on hydration of B-, A-, and Z-DNA. *Biopolymers.* 1990;30:649-656.
4. Shinyashiki N, Asaka N, Mashimo S, et al. Microwave dielectric study on hydration of moist collagen. *Biopolymers.* 1990;29:1185-1191.
5. Miura N, Asaka N, Shinyashiki N, et al. Microwave dielectric study on bound water of globule proteins in aqueous solution. *Biopolymers.* 1994;34:357-364.
6. Miura N, Hayashi Y, Shinyashiki N, et al. Observation of unfreezable water in aqueous solution of globule protein by microwave dielectric measurement. *Biopolymers.* 1995;36:9-16.
7. Miura N, Hayashi Y, Mashimo S. Hinge-bending deformation of enzyme observed by microwave dielectric measurement. *Biopolymers.* 1996;39:183-187.
8. Hayashi Y, Miura N, Isobe J, et al. Molecular dynamics of hinge-bending motion of IgG vanishing with hydrolysis by papain. *Biophys J.* 2000;79:1023-1029.
9. Boireau-Adamezyk E, Baillet-Guffroy A, Stamatias GN. Mobility of water molecules in the stratum corneum: effects of age and chronic exposure to the environment. *J Invest Dermatol.* 2014;134:2046-2049.
10. Kaaze U. Complex permittivity of water as a function of frequency and temperature. *J Chem Eng Data.* 1989;34:371-374.
11. Buchner R, Barthel J, Stauber J. The dielectric relaxation of water between 0°C and 35°C. *Chem Phys Lett.* 1999;306:57-63.
12. Fukasawa T, Sato T, Watanabe J, et al. Relation between dielectric and low-frequency Raman spectra of hydrogen-bond liquids. *Phys Rev Lett.* 2005;95:1-4.
13. Schrodle S, Hefter G, Buchner R. Dielectric spectroscopy of hydrogen bond dynamics and microheterogeneity of water-dioxane mixtures. *J Phys Chem.* 2007;111:5946-5955.

14. Tagami H, Ohi M, Iwatsuki K, et al. Evaluation of skin surface hydration in vivo by electrical measurement. *J Invest Dermatol.* 1980;75:500-507.
15. Naito S. A new method of measuring stratum corneum water content by dielectric analysis in microwave region. *J Jpn Cosmet Sci Soc.* 1998;22:1-7.
16. Mayrovitz HN, Bernal M, Brilit F, et al. Biophysical measures of skin tissue water: variations within and among anatomical sites and correlations between measures. *Skin Res Technol.* 2013;19:47-54.
17. Pratchyapruit W, Kikuchi K, Gritiyarangsana P, et al. Functional analyses of the eyelid skin constituting the most soft and smooth area on the face: contribution of its remarkably large superficial corneocytes to effective water-holding capacity of the stratum corneum. *Skin Res Technol.* 2007;13:169-175.
18. Naito S, Hoshi M, Mashimo S. A method of measuring surface permittivity by microwave dielectric analysis. *Rev Sci Instrum.* 1996;67:3633-3641.
19. Naito S, Hoshi M, Yagihara S. Microwave dielectric analysis of human stratum corneum in vivo. *Biochim Biophys Acta.* 1998;1381:293-304.
20. Hayashi Y, Miura N, Shinyashiki N, et al. Free water content and monitoring of healing processes of skin burns studied by microwave dielectric spectroscopy in vivo. *Phys Med Biol.* 2005;50:599-612.
21. Hashimoto T, Yamamura M, Yagihara S, et al. Build up of the epidermis after excise. *Tokai J Sports Med Sci.* 2003;15:67-72.
22. Hirao T, Egawa M, Yamashita T. Recent advances in technologies for measurement of the skin. *J Surf Sci Soc Jpn.* 2014;35:17-22.
23. Sato S, Maruyama Y, Kamata H, et al. Evaluation of water measurement techniques for human skin by dielectric spectroscopy and confocal Raman spectroscopy. *Trans Mat Res Soc Jpn.* 2015;40:133-136.
24. Hashimoto M, Goto T, Shinyashiki N, et al. Interpretation of hydration structure of human skin from analysis of electrodes used in dielectric spectroscopy. *Tokai J Sports Med Sci.* 2007;19:52-62.
25. Goto T, Hashimoto M, Shinyashiki N, et al. Dielectric study on distribution of water in human skin. *Trans Mat Res Soc Jpn.* 2006;31:771-774.
26. Barthel J, Buchner R. High frequency permittivity and its use in the investigation of solution properties. *Pure Appl Chem.* 1991;63:1473-1482.
27. Cole RH. Evaluation of dielectric behavior by time-domain spectroscopy. I. Dielectric response by real time analysis. *J Phys Chem.* 1975;79:1459-1469.
28. Cole RH. Evaluation of dielectric behavior by time-domain spectroscopy. II. Complex permittivity. *J Phys Chem.* 1975;79:1469-1474.
29. Cole RH, Mashimo S, Winsor P IV. Evaluation of dielectric behavior by time-domain spectroscopy. 3. precision difference methods. *J Phys Chem.* 1980;84:786-793.
30. Nakamura H, Mashimo S, Wada A. Application of time-domain reflectometry covering a wide frequency range to the dielectric study of polymer solutions. *J App Phys.* 1982;21:467-474.
31. Nakamura H, Mashimo S, Wada A. Precise and easy method of TDR to obtain dielectric relaxation spectra in GHz region. *J App Phys.* 1982;21:1022-1024.
32. Yazawa S. Comparative study of skin tissue in various parts of human body. *Med Res.* 1933;7:1805-1846.

How to cite this article: Maruyama Y, Kamata H, Watanabe S, Kita R, Shinyashiki N, Yagihara S. Electric-field penetration depth and dielectric spectroscopy observations of human skin. *Skin Res Technol.* 2020;26:255-262. <https://doi.org/10.1111/srt.12788>